AJNR

This information is current as of July 25, 2025.

Deep Learning Denoising Improves CT Perfusion Image Quality in the Setting of Lower Contrast Dosing: A Feasibility Study

Mahmud Mossa-Basha, Chengcheng Zhu, Tanya Pandhi, Steve Mendoza, Javid Azadbakht, Ahmed Safwat, Dean Homen, Carlos Zamora, Dinesh Kumar Gnanasekaran, Ruiyue Peng, Steven Cen, Vinay Duddalwar, Jeffry R. Alger and Danny J.J. Wang

Deep Learning Denoising Improves CT Perfusion Image Quality in the Setting of Lower Contrast Dosing: A Feasibility Study

Mahmud Mossa-Basha, Chengcheng Zhu, Tanya Pandhi, Steve Mendoza, Javid Azadbakht, Ahmed Safwat, Dean Homen, Carlos Zamora, Dinesh Kumar Gnanasekaran, Ruiyue Peng, Steven Cen, Vinay Duddalwar, Jeffry R. Alger, and Danny J.J. Wang

ABSTRACT

BACKGROUND AND PURPOSE: Considering recent iodinated contrast shortages and a focus on reducing waste, developing protocols with lower contrast dosing while maintaining image quality through artificial intelligence is needed. This study compared reduced iodinated contrast media and standard dose CTP acquisitions, and the impact of deep learning denoising on CTP image quality in preclinical and clinical studies. The effect of reduced X-ray mAs dose was also investigated in preclinical studies.

MATERIALS AND METHODS: Twelve swine underwent 9 CTP examinations each, performed at combinations of 3 different x-ray (37, 67, and 127 mAs) and iodinated contrast media doses (10, 15, and 20 mL). Clinical CTP acquisitions performed before and during the iodinated contrast media shortage and protocol change (from 40 to 30 mL) were retrospectively included. Eleven patients with reduced iodinated contrast media dosages and 11 propensity-score-matched controls with the standard iodinated contrast media dosages were included. A residual encoder-decoder convolutional neural network (RED-CNN) was trained for CTP denoising using *k*-space-weighted image average filtered CTP images as the target. The standard, RED-CNN-denoised, and *k*-space-weighted image average noise-filtered images for animal and human studies were compared for quantitative SNR and qualitative image evaluation.

RESULTS: The SNR of animal CTP images decreased with reductions in iodinated contrast media and milliampere-second doses. Contrast dose reduction had a greater effect on SNR than milliampere-second reduction. Noise-filtering by *k*-space-weighted image average and RED-CNN denoising progressively improved the SNR of CTP maps, with RED-CNN resulting in the highest SNR. The SNR of clinical CTP images was generally lower with a reduced iodinated contrast media dose, which was improved by the *k*-space-weighted image average and RED-CNN denoising ($P < .05$). Qualitative readings consistently rated RED-CNN denoised CTP as the best quality, followed by *k*-space-weighted image average and then standard CTP images.

CONCLUSIONS: Deep learning-denoising can improve image quality for low iodinated contrast media CTP protocols, and could approximate standard iodinated contrast media dose CTP, in addition to potentially improving image quality for low milliampere-second acquisitions.

ABBREVIATIONS: AI = artificial intelligence; DL = deep learning; ICM = iodinated contrast media; KWIA = *k*-space-weighted image average; LCD = low contrast dose; PSNR = peak SNR; RED-CNN = residual encoder-decoder convolutional neural network; RMSE = root mean square error; SCD = standard contrast dose; SSIM = structural similarity index measure

A coronavirus 2019 (COVID-19) outbreak in Shanghai, China in 2022 resulted in shutdown of an iohexol iodinated contrast manufacturing facility, leading to a global shortage of iodinated contrast media (ICM). Considering that iohexol represented 50% of ICM use in the United States and most institutions rely on single agents, this resulted in many institutions scrambling for workflow solutions to the prolonged shortage that extended from late spring through the summer.[1,2] There were many solutions considered or implemented by institutions to conserve the ICM supply, including reduction in ICM dosing for imaging examinations.[1]

Table 1: CTP imaging parameters for animal and patient studies

	Animal Study	Patient Study
Scanner	Aquilion ONE	Somatom Force Dual Energy or Definition AS 128-section
No. of slices	8	22 or 11[a]
Tube voltage (kVp)	80	70
Tube current (mAs)	127, 67, 37	200
Cycle time (s)	2	1.5
Scan duration (s)	60	45
Section thickness (mm)	5	5
Pixel spacing (mm^2)	0.47 × 0.47	0.47 × 0.47
Reconstructed image size	512 × 512	512 × 512
Axial coverage (mm)	240	240
Contrast (mL)	10, 15, 20 (iopamidol)	40 or 30 (iohexol)

[a] Slices acquired differed between scanners due to technical capabilities, to maintain equivalent temporal resolution.

In current practice, reduction of ICM dosing used in radiologic imaging while maintaining image quality has the benefit of reducing the amount of ICM contaminants reaching water sources and systems and potentially reducing the toxic ICM metabolites that have a negative impact on aquatic environments and human drinking water.[3] Additional practice benefits include reduced ICM waste, cost, and dose-dependent adverse ICM effects.

CTP has become a validated imaging technique for stroke intervention,[4-6] along with NCCT head and CTA head and neck examinations. CTP, however, has a low SNR[7] in addition to other potential artifacts,[8] and ICM dose reduction carries the risk of further image degradation. Deep learning (DL)-enabled noise reduction has been developed for various imaging modalities, including CT and MR imaging, to accelerate imaging for improved throughput and reduced radiation or to improve spatial or temporal resolution.[9,10] Artificial intelligence (AI) processing and enhancement of CTP with lower ICM dosing has the potential to improve image quality and maintain the diagnostic performance of CTP. In this study, we evaluated qualitative and quantitative image quality of CTP maps from standard and reduced ICM-dose CTP acquisitions, specifically comparing standard, DL-denoised and noise-filtered images using a *k*-space-weighted image average (KWIA)[11] in clinical studies and the combination of different levels of ICM dosing and milliampere-second for the same comparison in preclinical animal models. We hypothesized that DL-denoising reconstruction can enhance image quality in low contrast dose (LCD) CTP acquisitions to approximate that of the standard contrast dose (SCD) in human studies and similarly improve image quality in swine CTP acquisitions with reduced milliampere-second and LCD.

MATERIALS AND METHODS
Animal Studies
Following Institutional Animal Care and Use Committees approval at the University of Southern California, 12 swine (male, age 4.3 [SD, 0.4] months; weight, 19.4 [SD, 1.6] kg) were scanned on an Aquilion ONE CT scanner (Canon Medical Systems) using a clinical CTP protocol (80 kV[peak], 30 frames with a 2-second cycle time, 8 × 5 mm slices; Table 1). Each scan was started with a 1-second postinjection delay following iopamidol (Isovue-370; Bracco Diagnostics) administration at a 2.5-mL/s flow rate, followed by a 20-mL saline flush. The CTP protocol was a standard clinical protocol, with contrast dose

and flow rate halved considering the animal size relative to human size. The animals underwent 9 CTP examinations each, performed at combinations of 3 different milliampere-second values (37, 67, and 127 mAs) and 3 different contrast doses (10, 15, and 20 mL). The milliampere-second values were almost doubled between each value (37 to 67, 67 to 127) to provide a wide coverage from low-to-standard doses. Each scan with 1-minute duration was performed in randomized order, and there were 5-minute gaps between scans. The detailed animal preparation and anesthesia procedures are listed in the Online Supplemental Data. The goal of the animal study was to investigate the effect of different degrees and combinations of reduced contrast and milliampere-second values on CTP parametric map image quality.

Patient Population
At a second institution, after retrospective institutional review board approval with a waiver of informed consent, we queried the radiology data set for CTP performed for acute stroke evaluation, between February 1, 2022, and September 1, 2022, before and after the protocol change at the start of the ICM shortage. The University of North Carolina Medical Center reduced ICM dosing for CTP protocols by 25% (40 to 30 mL) on May 1, 2022. Inclusion criteria were the following: 1) adult patients older than 18 years of age, and 2) having undergone CTP for stroke evaluation. Exclusion criteria were the following: 1) poor image quality, and 2) prior craniotomy or cerebral hemorrhage that may degrade CTP image quality or performance. A total of 65 subjects with standard ICM doses and 18 patients with reduced ICM dosage were reviewed. From these, 11 subjects with reduced ICM doses were selected after excluding those younger than 18 years of age ($n = 2$) and those being evaluated for complications of aneurysmal subarachnoid hemorrhage ($n = 5$). Then, 11 propensity-matched patients with a standard ICM dosage (age, 77 [SD, 18] years; 5 men) were selected to compare with the 11 patients with reduced ICM dosages (age 77 [SD, 11] years; 7 men). Propensity score matching included patient age, sex, body mass index, and acute infarction presence to limit patient-specific confounders (see the Online Supplemental Data for demographic and clinical information). The goal of the clinical study was to evaluate the effect of LCD on CTP parametric map image quality on 2 closely matched patient cohorts. The study's external validation of the algorithm provides Level 5A evidence.

Clinical CTP Protocol
CT stroke imaging was performed on Somatom Force dual-energy or Definition AS 128-section (Siemens) scanners. Scans were obtained in helical mode. Patients were placed in a supine position with the chin down. A Coban 2-layer compression system (3M) was used to wrap the head to reduce head motion. CTP was performed with 200 mAs and 70 kVp, with 30 timeframes and 1.5-second temporal resolution, for a total acquisition time of 45 seconds (Table 1).

Before protocol modification due to the ICM shortage, the SCD protocol was 40 mL of iohexol (Omnipaque 350; GE Healthcare) at 6-mL/s IV contrast injection, followed by a 50-mL saline chaser. The LCD protocol was 30 mL of iohexol 350 at 6-mL/s IV contrast injection followed by a 50-mL saline chaser.[2]

Image Preprocessing

For the animal study, CTP scans with excessive motion (>3 mm in any direction between frames) and/or extravasation were excluded, resulting in a total of 72 CTP scans from 12 swine. For the clinical study, all 22 CTP scans passed quality control. The standard DICOM images of both animal and clinical studies were processed using the KWIA[11] method (Hura CTP software; Hura Imaging), which is a robust algorithm that applies spatiotemporal filtering in the spatial frequency domain to reduce CTP image noise.

DL Algorithm

A residual encoder-decoder convolutional neural network (RED-CNN)[12] was used as the DL algorithm for CTP denoising, given its favorable performance in noise suppression, structural preservation, and lesion detection compared with other denoising algorithms.[13] For the clinical study, the RED-CNN was pretrained on 120 CTP data sets from 4 manufacturers (Siemens, Canon, GE Healthcare, and Philips Healthcare, with an equal ratio of images) as the input (scanners and protocol parameters are listed in the Online Supplemental Data), with the corresponding KWIA-filtered CTP images as the target. The model input and output were single time frame CTP images of 512 × 512. The 120 pretraining CTP data set was split with an 80:20 train/test distribution for training and testing, and the model was trained on a multigraphics processing unit (GPU with two Titan RTX video graphics cards; Nvidia) workstation using a DataParallel mechanism (PyTorch), with an Adam optimizer with learning rate decay from $1e^{-3}$ to $1e^{-5}$ after every 35,000 iterations, and the loss function was defined as

$$Loss = Loss_{L1} + Loss_{L2} + \lambda \cdot Loss_{perceptual},$$

where $Loss_{L1}$ and $Loss_{L2}$ are L1 (mean absolute error) and L2 loss (root mean square error) respectively, and $Loss_{perceptual}$ is a perceptual loss between the predicted and target images with the weighting $\lambda = 0.001$. The perceptual loss function used a pretrained VGG-16 network (Visual Geometry Group) to analyze both the target image and the image the model created. The performance of RED-CNN was measured on the basis of peak SNR (PSNR), structural similarity index measure (SSIM), and root mean square error (RMSE) metrics. The pretrained RED-CNN was then fine-tuned on the 22 clinical CTP data sets (11 LCD, 11 SCD) with 11-fold cross-validation.

For the animal study, the RED-CNN was trained from scratch using the original animal CTP images as the input, and the corresponding KWIA-filtered CTP images as the target, with 12-fold cross-validation. The hyperparameters, training, and evaluation of the RED-CNN generally followed those of a human study with fine-tuning in animal data sets. The swine CTP image was cropped to 180 × 180 to include the swine brain. The Online Supplemental Data illustrate the diagram of KWIA filtering and RED-CNN architecture.

Table 2: Performance metrics of RED-CNN denoising of human and swine CTP data for average milliampere-second values

	Standard Data	Predict
Human data		
Mean RMSE	9.190	8.452
Mean PSNR	35.017	35.830
Mean SSIM	0.990	0.995
Swine data		
Mean RMSE	2.002	1.686
Mean PSNR	46.724	48.712
Mean SSIM	0.993	0.996

Quantitative and Qualitative Evaluation

Postprocessing of CTP images was performed using Python implementation of the SCAN4 software,[14] which has been used in clinical trials.[15] Multiparametric perfusion maps including CBF, CBV, and MTT were generated using standard, noise-filtered (by KWIA algorithm), and DL-denoised (by RED-CNN) CTP images, respectively. The delay-insensitive block-circulant singular-value decomposition method was applied with a cutoff of 15% for singular values.[16] ROIs in gray and white matter were manually drawn on original CTP images by an experienced reader (J.R.A., Online Supplemental Data for representative ROIs and time courses of arterial input function, venous outflow function, gray and white matter). The SNR was calculated as the mean divided by the SD of ROI voxels.

In addition, 2 radiologists (with 4 and 6 years of experience reading CTP) performed ratings of image quality of CBF, CBV, and MTT maps independently and blinded to postprocessing methods. The ratings were done side-by-side-by-side, with ratings from 1 (best), 2 (good), to 3 (worst) for each method (RED-CNN, KWIA, standard) and for CBF, CBV and MTT maps of each subject, respectively.

Statistical Analysis

A hierarchical model with generalized estimating equations was used to make comparison between filtering methods by each dose level under each combination of ROI and perfusion parameters, by considering the repeat measures nested within the subject. For the comparison across methods or dose levels, the Tukey test was used to adjust the P value from multiple comparisons. Finally, the sensitivity analyses using the Wilcoxon rank score were conducted to confirm that the conclusions were not biased by the data-normality assumption violation. The weighted κ was used to assess the interrater agreement. SAS 9.4 (SAS Institute) was used for all statistical analyses.

RESULTS
Animal CTP Findings

The average performance metrics of animal (and clinical) RED-CNN models are listed in Table 2. As shown in representative CBF, CBV, and MTT maps (Online Supplemental Data) and corresponding SNR bar charts for gray and white matter respectively (Online Supplemental Data), there was a significant SNR reduction of the CBF map in white matter ($P = .02$) and SNR reduction of CBV ($P = .003$ and .002) and MTT ($P = .05$ and .04) maps in both gray and white matter with reductions in milliampere-second (Table 3). In addition, there was a reduction in CBF SNR

Table 3: Mean (95% CI) of SNR of CBF, CBV, and MTT maps in gray and white matter at 3 levels of mAs

ROI	Parameter	37 mAs	67 mAs	127 mAs	P Value
GM	CBF	1.98 (1.8– 2.2)	2.09 (1.9–2.3)	2.48 (1.8–3.2)	.11
GM	CBV	0.67 (0.5–0.8)	0.96 (0.7–1.2)	1.71 (1–2.4)	.003
GM	MTT	1.27 (1.1–1.4)	1.54 (1.3–1.8)	2.4 (1.4–3.3)	.05
WM	CBF	1.96 (1.8–2.1)	2.11 (1.9–2.3)	2.51 (1.8–3.2)	.02
WM	CBV	0.64 (0.5–0.8)	0.96 (0.7–1.2)	1.72 (1–2.4)	.002
WM	MTT	1.26 (1.1–1.5)	1.57 (1.3–1.8)	2.36 (1.4–3.3)	.04

Table 4: Mean (95% CI) of SNR of CBF, CBV, and MTT maps in gray and white matter at 3 levels of ICM dose

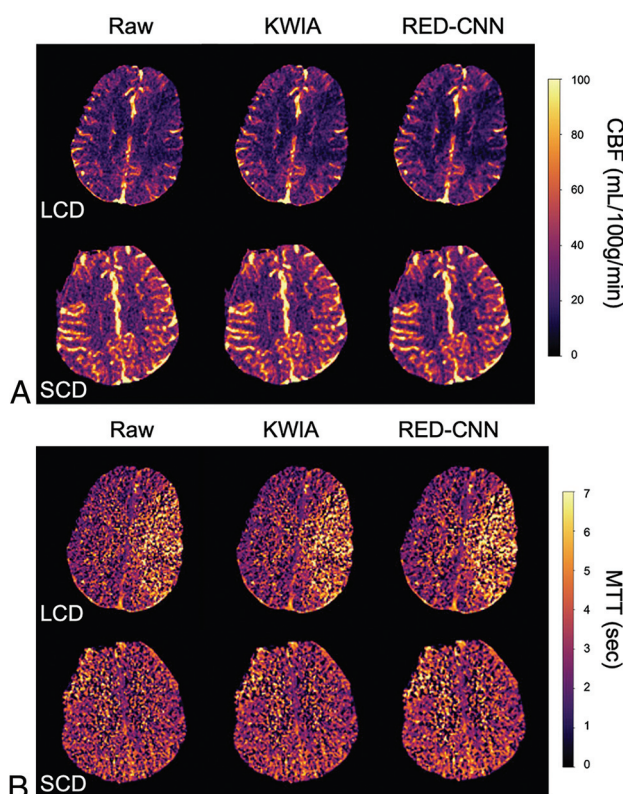| ROI	Parameter	ICM Dose 10 mL	ICM Dose 15 mL	ICM Dose 20 mL	P Value
GM	CBF	1.68 (1.3–2.1)	2.01 (1.6–2.4)	2.41 (1.8–3)	.01
GM	CBV	0.42 (0–0.9)	0.75 (0.4–1.1)	1.47 (0.9–2.1)	.09
GM	MTT	0.97 (0.4–1.5)	1.39 (1–1.8)	2.1 (1.4–2.8)	.13
WM	CBF	1.65 (1.2–2.1)	2 (1.6–2.4)	2.44 (1.8–3.1)	.002
WM	CBV	0.42 (0–0.9)	0.74 (0.4–1)	1.45 (0.9–2)	.09
WM	MTT	1 (0.5–1.5)	1.38 (1–1.8)	2.09 (1.3–2.8)	.16

FIG 1. CTP maps of 67-year-old man with left M1 MCA occlusion on CTA, presenting with right-sided weakness (LCD), and 61-year-old man with right MCA occlusion on CTA and left-sided weakness (SCD). Standard, KWIA-filtered, and RED-CNN denoised clinical CBF maps of representative LCD and SCD (A) and MTT maps of the same 2 patients (B), showing progressive, improved SNR with KWIA filtering and RED-CNN denoising, respectively.

in both gray and white matter with ICM dose reduction (Table 4). The SNR of CBV and MTT maps also decreased with milliampere-second but did not reach significance. The combination of 12-mAs x-ray and 20-mL contrast dose had the highest SNR, followed by 127-mAs x-ray and 15-mL contrast, and then 67-mAs x-ray and a 20-mL contrast. Contrast dose reduction had a greater effect on the SNR than milliampere-second reduction (50% contrast SNR is <25% mAs SNR). Noise-filtering by KWIA and DL-denoising by the RED-CNN progressively improved the SNR of CBF, CBV, and MTT maps ($P < .001$) (Online Supplemental Data). DL denoising by RED-CNN resulted in the highest SNR, though the improvement in SNR over KWIA was only significant for gray matter CBF (Online Supplemental Data). For 127-mAs and 15-mL contrast (ie, 25% contrast reduction), the RED-CNN was able to increase the SNR of perfusion maps to be comparable with those of the full dose of 127-mAs x-ray and 20-mL contrast (Online Supplemental Data).

Furthermore, KWIA and RED-CNN did not significantly change the mean CBF, CBV, and MTT values in gray and white matter compared with those calculated from standard CTP data, except that the CBF value in white matter calculated using the RED-CNN was significantly lower than that of the standard data ($P = .002$, (Online Supplemental Data).

Patient Imaging Cohort
Included studies were performed between November 1, 2022, and July 3, 2022. There were 11 CTP scans obtained at LCD and 11 propensity score–matched control SCD scans included in the study. Patient clinical and demographic features are depicted in the Online Supplemental Data.

Quantitative Image Quality Comparison
Figure 1 shows CBF (A) and MTT (B) maps processed using the 3 methods in patients representative of LCD and SCD, respectively (corresponding CBV maps are shown in the Online Supplemental Data). The SNR bar charts of CBF, CBV, and MTT maps of LCD and SCD cases in gray (A) and white matter (B), respectively, are shown in the Online Supplemental Data In general, patients with LCDs showed reduced SNR compared with those with SCD, though only MTT SNR in gray matter was significantly reduced in patients with LCDs (Table 5). RED-CNN and KWIA improved the SNR of perfusion maps compared with the corresponding standard images, as shown in the Online Supplemental Data. For gray matter, the RED-CNN provided significantly higher SNR than standard images for CBV (2.34 versus 2.01, $P < .001$) and MTT (3.34 versus 2.8, $P < .001$). SNR was also significantly improved with the RED-CNN compared with KWIA for CBF (2.19 versus 2.05, $P = .02$), but not for CBV or MTT. The SNR was significantly higher for KWIA compared with

standard data for CBV (2.19 versus 2.01, $P = .04$) and MTT (3.18 versus 2.8, $P < .001$), but not for CBF (Online Supplemental Data).

For white matter, the RED-CNN provided significantly higher SNR compared with standard images for CBF (1.51 versus 1.36, $P = .003$), CBV (0.59 versus 0.36, $P < .001$), and MTT (1.14 versus 1.02, $P = .02$) (Online Supplemental Data). The RED-CNN did not provide significant SNR improvement over KWIA for any perfusion parameters but showed a trend for CBV (0.52 versus 0.36, $P = .08$). KWIA showed significant improvement in SNR over standard data for CBF (1.44 versus 1.36, $P < .001$) and CBV (0.52 versus 0.36, $P < .001$), but not MTT. Furthermore, KWIA and the RED-CNN did not change the mean CBF, CBV, and MTT values compared with those calculated from standard CTP data, except that the CBF value in white matter calculated using KWIA and the RED-CNN was significantly lower than that of the standard data ($P < .001$, Online Supplemental Data).

Qualitative Image Rating Comparison

The weighted κ between the 2 raters was 0.77 (95% CI, 0.7–0.84), and the average ratings of the 2 raters are shown in Fig 2. Individual ratings are shown in the Online Supplemental Data. Most ratings (>60%) of RED-CNN, KWIA and standard perfusion maps were 1 (best), 2 (good), and 3 (worst), respectively.

DISCUSSION

The current study highlights the impact of reduction in the ICM dosage on CTP imaging quality, as implemented at many institutions during the recent ICM shortage. In animal models, we found significant reductions in the SNR with a reduction in milliampere-second and/or the ICM dose. Contrast dose reduction had a greater effect on the SNR than milliampere-second

reduction. This outcome is because contrast has a linear relationship with SNR, while milliampere-second has a square root relationship (50% mAs yields a SNR reduction similar to a 75% ICM dose). In clinical scanning, as well as in animal scanning, DL was able to significantly increase gray and white matter SNR for all perfusion maps, compared with standard data acquisitions. There was also SNR improvement using DL-denoising compared with KWIA-filtered perfusion maps, though the SNR differences were not consistently significant. The lack of significant SNR difference however, is expected considering that the RED-CNN was trained on KWIA-filtered maps as the reference standard for image quality. Qualitative evaluation also consistently rated RED-CNN denoised perfusion maps as having the best quality, followed by KWIA-filtered and then standard data. Furthermore, RED-CNN and KWIA denoising did not alter quantitative perfusion values in gray and white matter compared with those calculated from standard data, except for white matter CBF, which was reduced using the RED-CNN in both animal and clinical studies. This observation is consistent with literature showing overestimation of low perfusion values with noisy CTP data, which improves with denoising.[17]

These findings support DL-denoised CTP maps not only improving image quality in the setting of reduced ICM dose but also preserving or even improving quantification results of CTP. This outcome has advantages in terms of potentially permanently using protocols with lower ICM dosing to reduce ICM waste, reduce costs, limit drinking water contamination,[18] and potentially reduce the adverse dose-dependent effects of ICM.[19,20] This study also provides a pathway for further clinical evaluation for image-quality adequacy of DL-denoising applications to LCD and reduced milliampere-second CTP protocols in future human studies. With further validation, incorporation of low ICM dose protocols with DL-denoising reconstruction should advance clinical practice. With the animal data as a starting point, human CTP protocols with targeted reduced milliampere-second and ICM combined with DL-denoising reconstruction can be evaluated in humans to reduce patient exposures while maintaining diagnostic image quality.

AI and DL applications are impacting radiology clinical workflows and aiding clinical interpretations and triage decisions, including in stroke evaluation, with at least 22 FDA-approved stroke-related imaging algorithms;[21] however, none of these

Table 5: Mean (95% CI) SNR of 11 patients with LCD and 11 patients with SCD

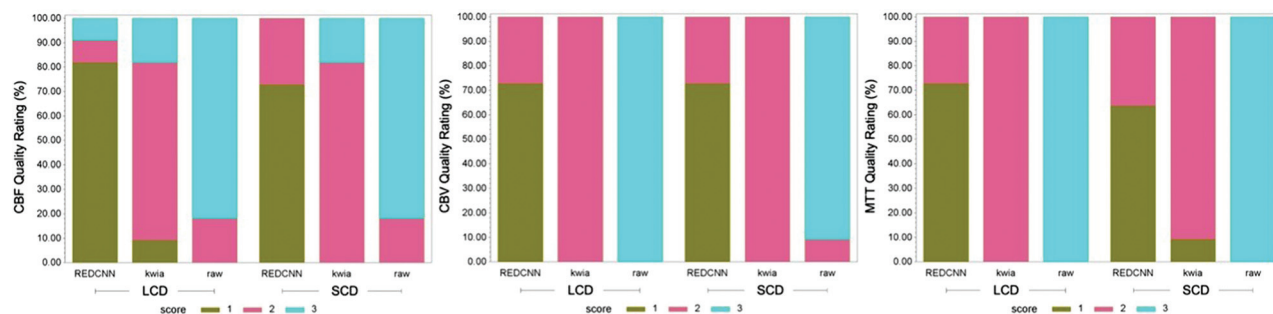| ROI	Parameter	LCD	SCD	P Value
GM	CBF	2.1 (2–2.2)	2.09 (1.8–2.4)	.94
GM	CBV	2.03 (1.8–2.3)	2.33 (2–2.7)	.13
GM	MTT	2.56 (2.1–3.1)	3.64 (2.8–4.5)	.03
WM	CBF	1.37 (1.2–1.5)	1.5 (1.4–1.6)	.14
WM	CBV	0.46 (0.3–0.6)	0.52 (0.4–0.7)	.54
WM	MTT	1.04 (1–1.1)	1.12 (1–1.2)	.23

FIG 2. Quality ratings of CBF, CBV, and MTT maps generated using RED-CNN, KWIA, and standard CTP data, comparing LCD and SCD. A rating of 1 was the best image quality, while 3 was the worst. The RED-CNN was consistently rated as 1 by 2 reviewers for all perfusion maps, KWIA primarily 2, and standard as 3, respectively. For 18.2% of ratings (36/198) with discrepancies between raters, the average score was rounded up to the nearest whole digit.

approved tools perform CTP denoising, to our knowledge. DL-denoising tools are also proliferating for image-quality improvement for other CT imaging applications, specifically to improve image quality and/or reduce radiation, and, for MR imaging applications, to reduce scan time[22] and increase spatial or temporal resolution.

An investigational 3D generative adversarial network algorithm reconstructed simulated reduced-dose CTP data, producing improved or equivalent image quality compared with the real data, with 50% and 25% of normal milliampere-second.[23] Other DL algorithms have shown the ability to restore temporally downsampled CTP data sets, to reduce milliampere-second,[24] or to interpolate missing temporal data.[25] These algorithms, however, did not address LCD CTP acquisitions and the resultant challenge of reduced SNR, which is unique to the current study.

Previous studies have developed non-DL-denoising algorithms for CTP image-quality improvement. Initial developments focused on improved image quality with low milliampere-second CTP protocols, with a reduction of noise by two-thirds.[26] With ultra-low-dose CTP (80% dose reduction), the combination of spatiotemporal filtering and quanta-stream diffusion for denoising was able to improve image quality relative to nondenoised CTP maps.[27] KWIA,[11] a low-dose CTP technique, using a projection view–shared averaging algorithm, averages the periphery of CTP *k*-space data with neighboring timeframes to improve the SNR, while normally sampling the center of *k*-space for maintenance of temporal resolution. The technique was able to maintain image quality, spatial and temporal resolution, and the accuracy of CTP quantification, compared with filtered back-projection reconstruction in phantom and human studies.

The novelty of the current study is the development of a DL-denoising algorithm for CTP image-quality enhancement. The DL-denoising model used in the current study was trained with KWIA-filtered maps as the reference standard for image quality, which effectively addresses the lack of reference images for CTP denoising due to ethical reasons. The DL-denoised perfusion maps had significantly higher SNR compared with KWIA for gray matter CBF ($P = .02$) and trended toward significance for white matter CBV maps ($P = .08$). In addition, the RED-CNN was better at preserving the fidelity of CTP time-series compared with KWIA, which showed temporal smoothing, especially for arterial input function (Online Supplemental Data). Overall, the RED-CNN outperformed KWIA for improving CTP image quality while preserving data fidelity, though the former was trained using the latter as the target.

There were several limitations to the current study. First, the sample size was small, limiting the comparisons made. Second, data collected were retrospective, potentially introducing confounders; however, we performed propensity score matching to mitigate this possibility. Third, the reduction in contrast dose between the LCD and SCD scans was only 25%, potentially limiting the resultant effect; however, the included animal data systematically addresses the impact of DL-denoising on both contrast and milliampere-second reductions. There are many alternative DL models that may outperform RED-CNN, including Transformers[28] and diffusion models, which can be investigated in future studies with larger patient data sets. Fourth, multiple consecutive ICM injections in the animal models could potentially impact quantitative evaluation due to increasing baseline contrast. Prior human studies, however, have indicated that there was no difference in quantitative CTP metrics, whether CTA was performed before or after the examination,[29] potentially indicating prior ICM doses would not affect CTP metrics. In addition, the order of CTP scans in the animal models was randomized to mitigate order bias.

CONCLUSIONS

DL-denoising can improve qualitative and quantitative image quality for CT perfusion compared with standard reconstruction algorithms. This feature can impact image quality for low iodinated contrast dose CTP protocols in human and animal scanning and could approximate standard contrast dose CT perfusion imaging.

REFERENCES

1. Grist TM, Canon CL, Fishman EK, et al. **Short-, mid-, and long-term strategies to manage the shortage of iohexol.** *Radiology* 2022;304:289–93 CrossRef Medline
2. Salazar G, Mossa-Basha M, Kohi MP, et al. **Short-term mitigation steps during the iohexol contrast shortage: a single institution's approach.** *J Am Coll Radiol* 2022;19:841–45 CrossRef Medline
3. Dekker HM, Stroomberg GJ, Prokop M. **Tackling the increasing contamination of the water supply by iodinated contrast media.** *Insights Imaging* 2022;13:30 CrossRef Medline
4. Albers GW, Marks MP, Kemp S, et al; DEFUSE 3 Investigators. **Thrombectomy for stroke at 6 to 16 hours with selection by perfusion imaging.** *N Engl J Med* 2018;378:708–18 CrossRef Medline
5. Nogueira RG, Jadhav AP, Haussen DC, et al; DAWN Trial Investigators. **Thrombectomy 6 to 24 hours after stroke with a mismatch between deficit and infarct.** *N Engl J Med* 2018;378:11–21 CrossRef Medline
6. Saver JL, Goyal M, Bonafe A, et al; SWIFT PRIME Investigators, **Stent-retriever thrombectomy after intravenous t-PA vs. t-PA alone in stroke.** *N Engl J Med* 2015;372:2285–95 CrossRef Medline
7. Schaefer PW, Souza L, Kamalian S, et al. **Limited reliability of computed tomographic perfusion acute infarct volume measurements compared with diffusion-weighted imaging in anterior circulation stroke.** *Stroke* 2015;46:419–24 CrossRef Medline
8. Hartman JB, Moran S, Zhu C, et al. **Use of CTA test dose to trigger a low cardiac output protocol improves acute stroke CTP data analyzed with RAPID software.** *AJNR Am J Neuroradiol* 2022;43:388–93 CrossRef Medline
9. Cao L, Liu X, Li J, et al. **A study of using a deep learning image reconstruction to improve the image quality of extremely low-dose contrast-enhanced abdominal CT for patients with hepatic lesions.** *Br J Radiol* 2021;94:20201086 CrossRef Medline
10. Liao S, Mo Z, Zeng M, et al. **Fast and low-dose medical imaging generation empowered by hybrid deep-learning and iterative reconstruction.** *Cell Rep Med* 2023;4:101119 CrossRef Medline

11. Zhao C, Martin T, Shao X, et al. **Low dose CT perfusion with k-space weighted image average (KWIA).** *IEEE Trans Med Imaging* 2020;39:3879–90 CrossRef Medline

12. Chen H, Zhang Y, Kalra MK, et al. **Low-dose CT with a residual encoder-decoder convolutional neural network.** *IEEE Trans Med Imaging* 2017;36:2524–35 CrossRef Medline

13. Du T, Zhang H, Li Y, et al. **Adaptive convolutional neural networks for accelerating magnetic resonance imaging via k-space data interpolation.** *Med Image Anal* 2021;72:102098 CrossRef Medline

14. Wang R, Yu S, Alger JR, et al. **Multi-delay arterial spin labeling perfusion MRI in moyamoya disease–comparison with CT perfusion imaging.** *Eur Radiol* 2014;24:1135–44 CrossRef Medline

15. Kidwell CS, Jahan R, Gornbein J, et al; MR RESCUE Investigators. **A trial of imaging selection and endovascular treatment for ischemic stroke.** *N Engl J Med* 2013;368:914–23 CrossRef Medline

16. Wintermark M, Maeder P, Thiran JP, et al. **Quantitative assessment of regional cerebral blood flows by perfusion CT studies at low injection rates: a critical review of the underlying theoretical models.** *Eur Radiol* 2001;11:1220–30 CrossRef Medline

17. Riordan AJ, Prokop M, Viergever MA, et al. **Validation of CT brain perfusion methods using a realistic dynamic head phantom.** *Med Phys* 2011;38:3212–21 .CrossRef Medline

18. Cheng X, Xia Y, Ji Q, et al. **Occurrence and risk of iodinated X-ray contrast media in source and tap water from Jiangsu province, China.** *J Hazard Mater* 2023;444:130399 CrossRef Medline

19. Koeppel DR, Boehm IB. **Shortage of iodinated contrast media: Status and possible chances: a systematic review.** *Eur J Radiol* 2023;164:110853 CrossRef Medline

20. Park HJ, Son JH, Kim TB, et al. **Relationship between lower dose and injection speed of iodinated contrast material for CT and acute hypersensitivity reactions: an observational study.** *Radiology* 2019;293:565–72 CrossRef Medline

21. Chandrabhatla AS, Kuo EA, Sokolowski JD, et al. **Artificial intelligence and machine learning in the diagnosis and management of stroke: a narrative review of United States Food and Drug Administration-approved technologies.** *J Clin Med* 2023;12:3755 CrossRef Medline

22. Rudie JD, Gleason T, Barkovich MJ, et al. **Clinical assessment of deep learning-based super-resolution for 3D volumetric brain MRI.** *Radiol Artif Intell* 2022;4:e210059 CrossRef Medline

23. Dashtbani Moghari M, Zhou L, Yu B, et al. **Efficient radiation dose reduction in whole-brain CT perfusion imaging using a 3D GAN: performance and clinical feasibility.** *Phys Med Biol* 2021;66 CrossRef Medline

24. Zhu H, Tong D, Zhang L, et al. **Temporally downsampled cerebral CT perfusion image restoration using deep residual learning.** *Int J Comput Assist Radiol Surg* 2020;15:193–201 CrossRef Medline

25. Dashtbani Moghari M, Sanaat A, Young N, et al. **Reduction of scan duration and radiation dose in cerebral CT perfusion imaging of acute stroke using a recurrent neural network.** *Phys Med Biol* 2023;68 CrossRef Medline

26. Sasaki T, Hanari T, Sasaki M, et al. **Reduction of radiation exposure in CT perfusion study using a quantum de-noising filter** [in Japanese]. *Nihon Hoshasen Gijutsu Gakkai Zasshi* 2004;60:1688–93 CrossRef Medline

27. Othman AE, Brockmann C, Yang Z, et al. **Impact of image denoising on image quality, quantitative parameters and sensitivity of ultra-low-dose volume perfusion CT imaging.** *Eur Radiol* 2016;26:167–74 CrossRef Medline

28. Shou Q, Zhao C, Shao X, et al. **Transformer-based deep learning denoising of single and multi-delay 3D arterial spin labeling.** *Magn Reson Med* 2023;91:803–18 CrossRef Medline

29. Morhard D, Wirth CD, Reiser MF, et al. **Optimal sequence timing of CT angiography and perfusion CT in patients with stroke.** *Eur J Radiol* 2013;82:e286–89 CrossRef Medline